



# Multiferroic Aurivillius-type $\text{Bi}_6\text{Fe}_{2-x}\text{Mn}_x\text{Ti}_3\text{O}_{18}$ ( $0 \leq x \leq 1.5$ ) ceramics with negative dielectric constant

Joanna A. Bartkowska<sup>1</sup> · Dariusz Bochenek<sup>1</sup> · Przemysław Niemiec<sup>1</sup>

Received: 22 June 2018 / Accepted: 11 November 2018 / Published online: 16 November 2018  
© The Author(s) 2018

## Abstract

Aurivillius-type ceramics  $\text{Bi}_6\text{Fe}_{2-x}\text{Mn}_x\text{Ti}_3\text{O}_{18}$   $x = 0, 0.3, 0.9, 1.5$  were obtained by a solid-state reaction method using high-purity  $\text{TiO}_2$ ,  $\text{Bi}_2\text{O}_3$ ,  $\text{Fe}_2\text{O}_3$  and  $\text{Mn}_2\text{O}_3$  powders. The milled powder was calcined at 1113 K for 4 h. After calcination, the powder was milled again than pressed into pellets and sintered at 1213 K for 4 h. It was detected that the addition of manganese ions to the multiferroic five-layer Aurivillius-type structure affects the size of the grains. It was found that, the certain amount of manganese ions causes that the polarization of the material doped by them, have the direction opposite to the direction of the applied electric field. The doped material behaves like dia-electric material. The presented research complements the research concerning the Aurivillius ceramics doped with manganese. An attempt was made to explain the reasons for the negative values of dielectric constant and dielectric loss, that occur in manganese-doped five-layer Aurivillius type ceramics and which have not been described in the literature so far.

## 1 Introduction

Multiferroics are materials in which at the same phase there are at least two ferroic features, i.e., ferroelectricity, ferromagnetism or ferroelasticity. The most interesting due to their potential applications are magnetoelectric multiferroic materials, i.e., materials that exhibit both magnetic and electrical properties. Magnetic and electric properties of multiferroic materials are coupling with each other. The existence of magnetoelectric coupling allows you to change the value of polarization, by an external magnetic field and there is a reverse phenomenon, i.e., an external electric field can affect the value of magnetization [1, 2]. In recent years, magnetoelectric multiferroic materials, which belong to the so-called bismuth oxides with perovskite-like layered structures, arouse great interest. The first description of perovskite-like layered structures was given by Aurivillius, hence often such materials are also called Aurivillius phases [3].

Aurivillius phases are described by the general chemical formula proposed by Subbaro  $(\text{Bi}_2\text{O}_2)^{2+}(\text{A}_{m-1}\text{B}_m\text{O}_{3m+1})^{2-}$  [4].

Despite many published papers presenting the results of research of multiferroic materials of Aurivillius-type, research on these structures is poorly advanced.

Multiferroic Aurivillius-type materials can find potential electronic and spintronic applications, for example as the random access memory [5, 6]. The interesting applications of ceramic materials that exhibit simultaneously magnetic, ferroelectric or ferroelastic ordering can be their use to make magnetic sensors, data storage, capacitor or digital memories [7–11].

An interesting material with an Aurivillius-type structure is five-layer  $\text{Bi}_5\text{Fe}_{2-x}\text{Mn}_x\text{Ti}_3\text{O}_{18}$  material doped with manganese. This material with  $0 \leq x \leq 0.8$  the first time was obtained by Zuo et al. [12]. Dielectric studies of this material showed negative values of the dielectric constant but authors did not pay attention to this fact. The reasons for the negative value of the dielectric constant in Aurivillius-type ceramics have not yet been thoroughly investigated and explained.

The subject of investigations that was presented in this paper were compounds which represent a structure with the unit cell consisting of one bismuth oxide layer  $(\text{Bi}_2\text{O}_2)^{2+}$  and five perovskite layers  $(\text{A}_{m-1}\text{B}_m\text{O}_{3m+1})^{2-}$  with a general chemical formula:  $\text{Bi}_5\text{Fe}_{2-x}\text{Mn}_x\text{Ti}_3\text{O}_{18}$ , where  $x = 0, 0.3, 0.9, 0.15$ .

✉ Joanna A. Bartkowska  
joanna.bartkowska@us.edu.pl

<sup>1</sup> Faculty of Computer Science and Materials Science, Institute of Technology and Mechatronics, University of Silesia in Katowice, 12, Żytnia St, 41-200 Sosnowiec, Poland

The aim of this work was obtain Aurivillius-type ceramics doped with manganese (Mn) ions and investigating its dielectric properties.

In this paper was presented conditions of the technological process of obtaining Aurivillius-type ceramics and results of researches the effect of manganese doping on its microstructure and dielectric properties.

## 2 Experimental

The Aurivillius-type  $\text{Bi}_6\text{Fe}_{2-x}\text{Mn}_x\text{Ti}_3\text{O}_{18}$  ceramics with  $x=0, 0.3, 0.9, 0.15$ , were prepared by conventional solid-state reaction from simple high-purity oxides:  $\text{Bi}_2\text{O}_3$  (99.999%, Sigma-Aldrich),  $\text{Fe}_2\text{O}_3$  (99.9%, Chempur),  $\text{Mn}_2\text{O}_3$  (99.9%, Sigma-Aldrich) and  $\text{TiO}_2$  (99.9%, Merck). The stoichiometric powder mixture was wet-milled in a planetary mill FRITSCH (Pulverisette-6) for 24 h in ethyl alcohol using zirconia-milling balls. After milling, powders were calcined at 1113 K/4 h. The calcined powders were milled again for 12 h and pressed into pellets of 10 mm in diameter and 1 mm in thickness under the pressure of 300 MPa. The pellets thus obtained were subjected to sintering at 1213 K/4 h.

For electric measurements, pellets were polished and platinum paste was applied on both surfaces as electrodes.

In the technological process discussed above, four Aurivillius-type ceramic materials with chemical formulas:  $\text{Bi}_5\text{Fe}_2\text{Ti}_3\text{O}_{18}$  (BFT),  $\text{Bi}_5\text{Fe}_{1.7}\text{Mn}_{0.3}\text{Ti}_3\text{O}_{18}$  (BFM3T),  $\text{Bi}_5\text{Fe}_{1.1}\text{Mn}_{0.9}\text{Ti}_3\text{O}_{18}$  (BFM9T) and  $\text{Bi}_5\text{Fe}_{0.5}\text{Mn}_{1.5}\text{Ti}_3\text{O}_{18}$  (BFM15T) were obtained.

X-ray measurements were carried out at room temperature using X'Pert-Pro PW3040/60 diffractometer. The copper radiations  $\text{CuK}_{\alpha 1/\alpha 2}$  were used. The X-ray diffraction patterns were stored at range of  $2\theta$  from  $5^\circ$  to  $140^\circ$  in step-scan mode: 0.05 degrees and 4 s/step. Microstructures of the fracture of obtained materials were characterized using a scanning electron microscope (JEOL JSM-7100F TTL LV). The chemical composition tests were performed by standard method, using an energy-dispersive spectrometer (EDS). The SEM/EDS tests were performed by the accelerating voltage 15–20 kV, low vacuum and with Au sputtering. The dielectric constant and the dielectric loss tangent were measured using LCR meter (QuadTech 1920 Precision) at temperature range from room temperature (RT) to 1050 K, for several frequencies of measurement field, range from 1 kHz to 1 MHz.

## 3 Results and discussion

### 3.1 Microstructure and chemical composition

Figure 1 presents comparison of the X-ray diffraction patterns, that were measured for the powder of

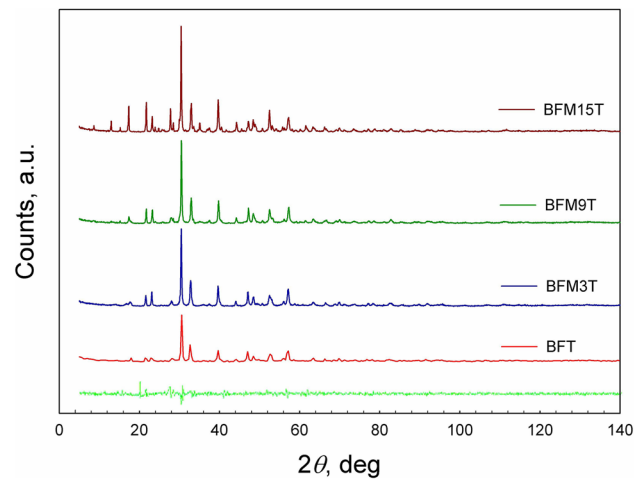


Fig. 1 X-ray spectra of BFT, BFM3T, BFM9T and BFM15T samples

Table 1 The lattice parameters and the volumes of the lattice cell for all studied BFT-type samples

	BFT	BFM3T	BFM9T	BFM15T
Space group	<i>Aba2</i>	<i>Aba2</i>	<i>Fmm2</i>	<i>Fmm2</i>
$a_0$ (nm)	0.54623	0.54482	4.09510	4.09277
$b_0$ (nm)	4.93447	4.93772	0.54334	5.4321
$c_0$ (nm)	0.54886	0.54705	0.54543	5.4549
Volume (nm <sup>3</sup> )	1.4794	1.4716	1.2136	1.2127

$\text{Bi}_6\text{Fe}_{2-x}\text{Mn}_x\text{Ti}_3\text{O}_{18}$  ceramics (with  $x=0, 0.3, 0.9, 0.15$ ). The X-diffraction lines, presented in the patterns were identified as a one belonging to the perovskite-like structure of Aurivillius-type. All the BFT-type materials were a single phase (rhombic system) without the presence of substrate phases or other equilibrium one. To determine the lattice parameters, the X-ray diffraction patterns were fitted using the Rietveld method [13]. In the case of the BFT and BFM3T samples the best fitting was obtained for the crystal structure, which belongs to the *Aba2* space group, while in the case of the BFM9T and BFM15T samples the best fitting was obtained for the *Fmm2* space group. Results of determined lattice parameters and volumes of the lattice cell are shown in Table 1.

The microscopic studies revealed some differences in the morphology of the surface of the sample fracture (after breaking the sample) of all investigated ceramic samples. The results of study, by scanning electron microscope, for undoped BFT sample and manganese-doped (BFM3T, BFM9T, BFM15T) ceramics are shown in Fig. 2a–d, respectively.

Microstructures of the surface of the sample fracture of all samples consist of platelet-like grains. Such a shape of grains is characteristic of bismuth perovskite-like layers

Aurivillius-type [14]. The fracture morphology of BFT ceramics (Fig. 2a) and BFM3T ceramics (Fig. 2b), which contains the smallest amount of manganese ions, compared to other investigated materials, are very similar.

Differences in the shape of grains and grain sizes are difficult to observe in SEM images (Fig. 2a, b) because both the shapes of the grains and grain sizes are very similar in both these materials. The experimental densities of BFT and BFM3T were determined and they are equal to  $7473 \text{ kg m}^{-3}$  and  $7314 \text{ kg m}^{-3}$ , respectively.

Further increasing the amount of manganese ions in Aurivillius-type ceramics (BFM9T sample) causes increase in the grain sizes (Fig. 2c). The experimental density of this ceramics is equal to  $6972 \text{ kg m}^{-3}$ .

A mixed nature of fractures occurs in BFT, BFM3T, BFM9T samples (Fig. 2a–c), that is the fractures occur both at grain boundaries and through grains.

The material with the largest amount of manganese ions, i.e., BFM15T sample, is characterized by large well-shaped grains, and the grain boundaries are clear. While the fracture along the grain boundaries is becoming dominating in this ceramic material (Fig. 2d). The experimental density of BFM15T sample was determined too, and it is equal to  $6250 \text{ kg m}^{-3}$ .

On the basis of the SEM examinations, it can be concluded that with increasing the amount of manganese, the grains were getting bigger. The calculated values of densities for all investigating  $\text{Bi}_6\text{Fe}_{2-x}\text{Mn}_x\text{Ti}_3\text{O}_{18}$  ceramic materials may indicate that an increased of the amount of manganese ions reduces the density of the Aurivillius-type ceramic material.

The EDS quantitative and qualitative analysis method was used to investigate the chemical composition of the Aurivillius-type ceramic materials. The EDS microanalysis of investigating materials qualitatively confirmed the assumed share of the individual components (Fig. 3a–d). The microanalysis of studied BFT, BFM3T, BFM9T and BFM15T ceramics was performed at micro-areas on the fractures of samples. Analyzed micro-areas are presented in interiors of Fig. 3a–d.

The EDS analysis of the element's distribution showed slight differences in the chemical composition of investigating ceramic materials. The percentage share of chemical elements in all samples was given in Table 2.

The quantitative analysis of the chemical composition of tested samples shown, that Ti ions are most stable in all tested ceramic samples. Their quantity is in the range from 0.94 to 0.97 of the initial value for BFT and BFM3T,

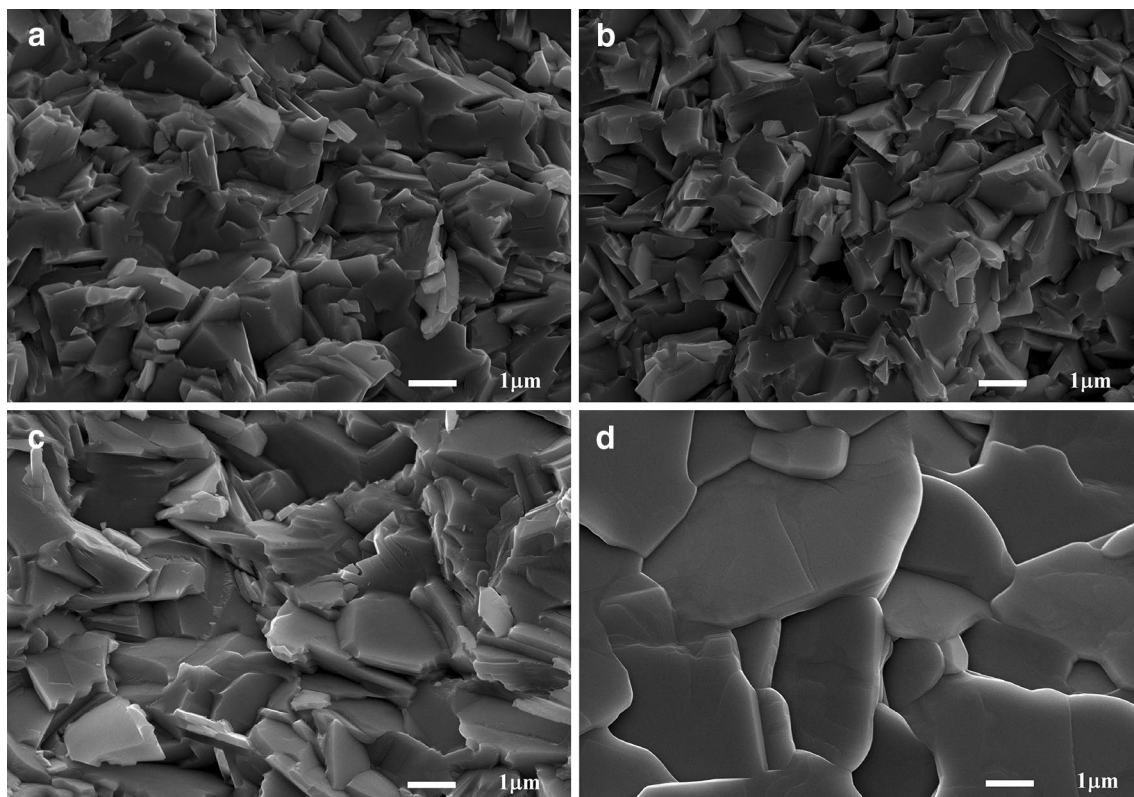


**Fig. 2** The SEM images of the microstructure of fracture surface of samples of Aurivillius-type ceramics undoped—BFT (a) and doped with manganese: BFM3T (b), BFM9T (c) and BFM15T (d)

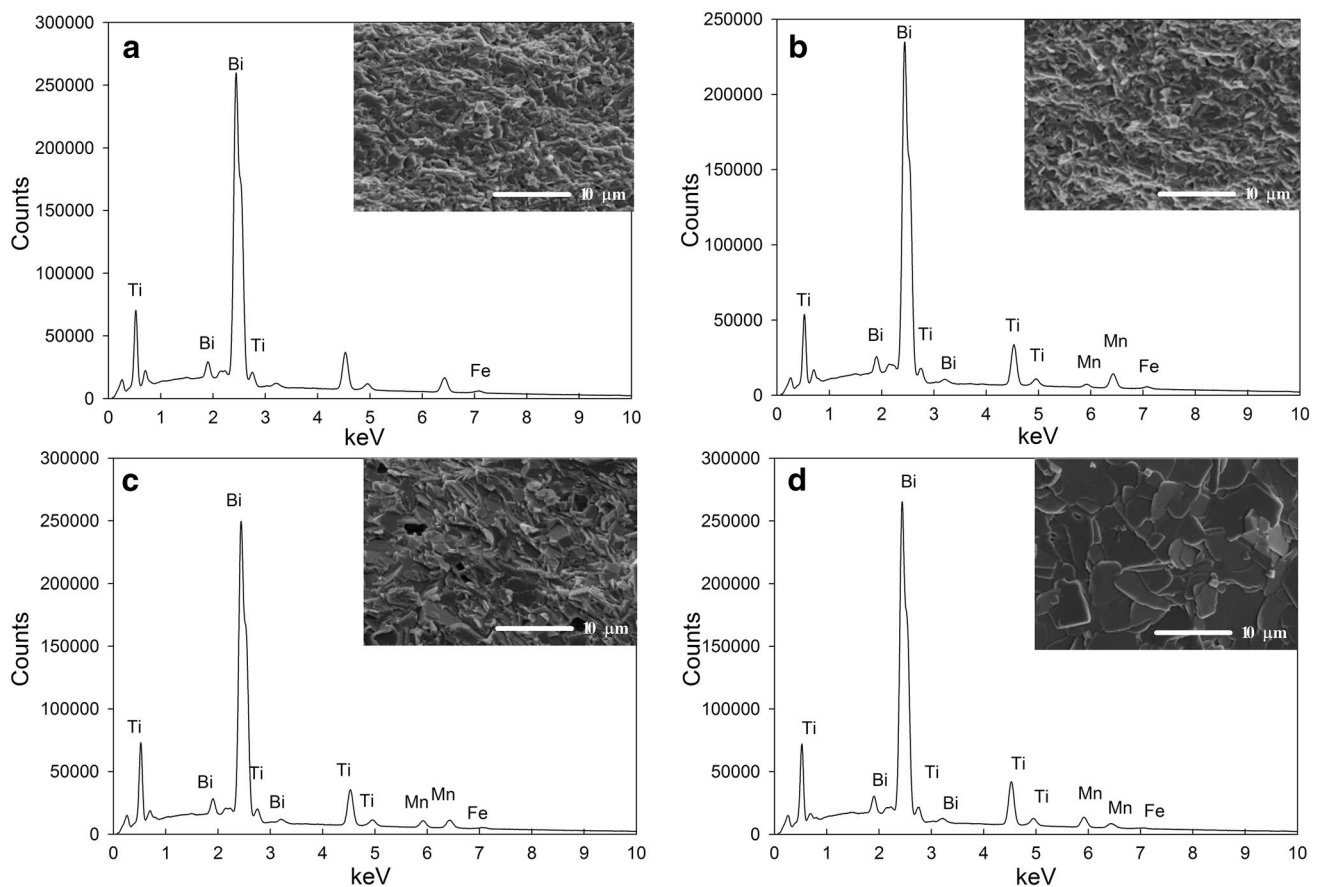


**Fig. 3** The EDS analysis of chemical elements of fracture surface of samples: undoped—BFT (a) and doped with manganese: BFM3T (b), BFM9T (c) and BFM15T (d), in micro-areas presented in interiors (a–d), respectively

respectively. The Mn ions content is on the level from 0.82 to 0.94 of the initial value for BFM9T and BFM15T, respectively. The quantity of Fe ions is at 0.84 of the initial value for BFM15T to 0.99 of the initial value for BFT. All deviations between the theoretical content of chemical elements in the tested samples and their real content are within the acceptable range.

### 3.2 The dielectric properties

The temperature dependencies of dielectric constant  $\epsilon'$  for BFT-type are shown in Fig. 4. In the case of the BFT (for  $x=0$ ) sample values of dielectric constant increase with increasing temperature as shown in the Fig. 4a. The first maximum (a sharp peak) of the dielectric constant appears at around 550 K (the interior of Fig. 4a).

These results correspond to the results of the research presented in the paper of Zuo et al. [12]. Zuo et al.

**Table 2** Theoretical and experimental percentage of chemical elements in all studied BFT-type samples

Chemical element	BFT		BFM3T		BFM9T		BFM15T	
	Theoretical (%)	Experimental (%)	Theoretical (%)	Experimental (%)	Theoretical (%)	Experimental (%)	Theoretical (%)	Experimental (%)
O	16.02	16.01	16.03	16.13	16.03	16.71	16.03	16.89
Ti	7.99	7.53	7.99	7.81	7.99	7.58	7.99	7.56
Bi	69.77	70.26	69.78	69.98	69.90	70.19	69.82	69.93
Fe	6.21	6.20	5.28	5.19	3.42	3.26	1.55	1.31
Mn	–	–	0.92	0.89	2.75	2.27	4.59	4.31

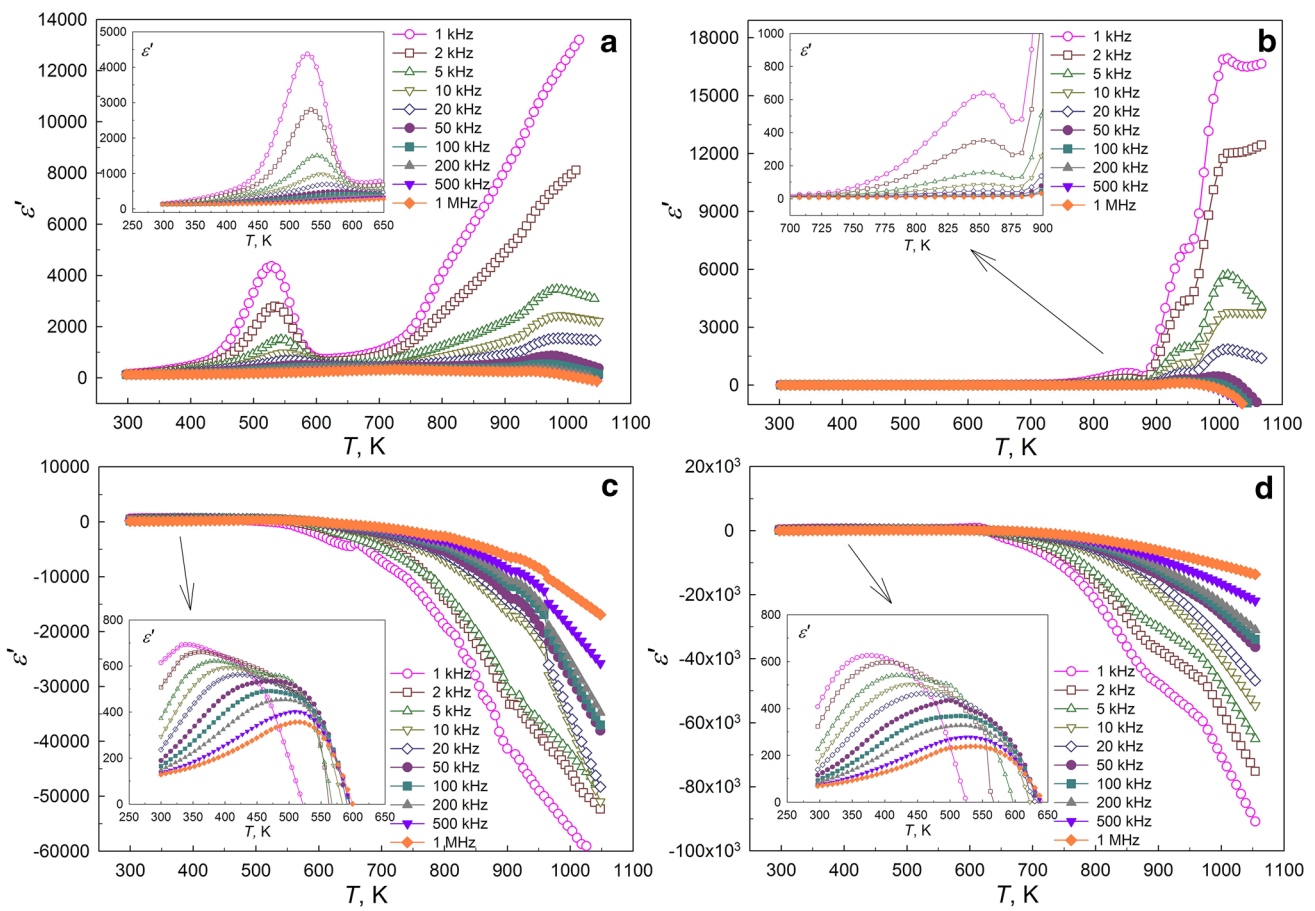


**Fig. 4** Temperature dependencies of dielectric constant for Aurivillius-type ceramic materials: undoped—BFT (a) and doped with manganese: BFM3T (b), BFM9T (c) and BFM15T (d)

obtained the analogous manganese-free ceramic material but in other than our technological conditions. Results of dielectric studies of BFT ceramic material (manganese free) obtained by Zuo et al. were shown an existence of weak maximum of dielectric constant, at about 570 K.

These results indicate the influence of technological conditions, such as temperature and time of calcination as well as sintering, on the dielectric properties of this Aurivillius-type material.

With the increase of the measuring field frequency, the location of this maximum is shifted towards higher temperatures. Namely it occurs in the temperature range from 550 to 750 K, for a measuring field frequency from 1 kHz to 1 MHz (it is not visible in Fig. 4a), respectively. The height of this maximum decreases with increase of the measuring field frequency. Thus, both the location and height of the first maximum depend on the frequency. The shift of the peak towards higher temperatures, for increasing frequency of measuring field, is a hallmark of the phenomenon of dielectric relaxation [15].

The source of the dielectric relaxation peak may be oxygen vacancies or variable oxidation of Fe ions [16]. The second maximum of the dielectric constant occurs at 950 K and its location does not depend on the frequency. That behavior is a normal for ferroelectric materials [17]. This maximum is related with the ferroelectric–paraelectric phase transition and the location of this maximum is the temperature of phase transition ( $T_m$ ) [18].

Figure 4b shows temperature dependencies of dielectric constant  $\epsilon'(T)$  for BFM3T ceramics. In the case of the BFM3T sample (for  $x=0.3$ ) the dielectric constant increases slowly with increasing temperature. The dielectric constants exhibit two maxima, the first one is at 850 K and the second one at 1000 K. The location the first maximum of the dielectric constant depends on the frequency. The dielectric relaxation processes are responsible for its occurrence, similarly as in the case of BFT material. The dielectric relaxation can be associated with the occurrence of oxygen vacancies or variable oxidation of Fe ions ( $\text{Fe}^{2+}/\text{Fe}^{3+}$ ) in BFM3T material. The location of the second maximum does not depend on

the frequency, while its height decreases with the increase in frequency of measurement field. This maximum may be related to the ferroelectric–paraelectric phase transition in this ceramic material. Fig. 4b shows, that at a certain temperature, the dielectric constant reaches negative values for several measuring field frequencies and so the negative values of dielectric constant appeared at 970 K (for frequency 1 MHz) and at 1030 K (for frequency to 50 kHz).

The dielectric constant for the sample BFM9T (where  $x=0.9$ ) exhibits a similar temperature dependence like sample with BFM3T, but the second maximum does not occur on the temperature dependence of dielectric constant (Fig. 4c). The maximum of dielectric constant for BFM9T occurs in the range from 325 K (for 1 kHz) to 550 K (for 1 MHz). This maximum depends on frequency of measurement field, and it shifts as the frequency increases towards higher temperatures. As shown in the Fig. 4c, the negative values of the dielectric constant appear above certain temperatures for all measuring field frequencies (i.e., 520 K for 1 kHz, 600 K for 1 MHz).

Figure 4d shows temperature dependencies of dielectric constant  $\epsilon'$  for BFM15T. The dielectric constant increases with increasing temperature and reach maximum at temperature 350 K (for 1 kHz) and 550 K (for 1 MHz). Further temperature rise, cause decrease of the dielectric constant to negative values. The local maximum of the dielectric constant depends on the frequency of the measurement field and it behaves like for BFM9T sample. The dependence of the maximum of the dielectric constant on the frequency may indicate the occurrence of dielectric relaxation processes in ceramic material [19]. The dielectric constant values of BFM15T ceramics, similar like the dielectric constant of BFM9T sample, reach negative values at different temperatures of different frequencies (e.g., 525 K for 1 kHz and 635 K for 1 MHz).

In measurement temperature range, negative values of dielectric constant appeared for three Aurivillius-type ceramic materials, namely BFM3T, BFM9T and BFM15T samples. Figure 4 shows, that the negative values of dielectric constant for BFM3T ceramics appears from about 970 K for 50 kHz and higher ones (Fig. 4b, inside). In cases of BFM9T (Fig. 4c, inside) and BFM15T (Fig. 4d, inside) samples, the negative values of dielectric constants occur for all range of frequencies. In the case of the BFM9T samples, the negative values of dielectric constants occur at 520 K, while for the BFM15T sample at 525 K. The negative values of the dielectric constant indicate a change in the electrical character of the investigating Aurivillius-type ceramic materials [20].

The applied external electric field causes an oscillating electron motion in ceramic material. If the electron oscillations are consistent with the direction of the applied external electric field, then the direction of the polarization

vector is consistent with the direction the applied electric field and the value of the dielectric constant is positive. Therefore, the negative value of the dielectric constant may indicate that the electron oscillations are opposite to the direction of the applied external electric field, i.e., the direction of polarization of this material is opposite to the direction of applied electric field.

Materials that behave in this way may be called dielectric materials by analogy to diamagnetic materials. This is related to the direction of the magnetization of diamagnetic materials which is opposite to the direction of applied external magnetic field [21].

The dielectric loss tangents ( $\tan \delta$ ) as a function of a temperature were measured for all tested ceramics and the results of these measurements are shown in Fig. 5. When comparing the results of the dielectric loss, it can be observed that BFT material features positive values of the dielectric loss tangent in the studied range of the temperature, and for all frequencies of measuring field (Fig. 5a). While BFM3T material shows positive values of the dielectric loss in the all range of the temperature only for frequencies up to 20 kHz. For higher frequencies, the negative dielectric loss, above a certain temperature are observed (Fig. 5b). Subsequent BFM9T and BFM15T materials, above the certain temperature, show the negative dielectric loss (Fig. 5c, d) for all measuring frequency. The negative dielectric loss may indicate that more energy is emitted than absorbed [22]. Because of the need to comply with the principle of energy conservation, there must be some mechanism in material that allows you to store energy and release it only at certain temperatures or/and frequencies. The negative dielectric loss can therefore be associated with the existence of uncompensated charges in the material. These charges can accumulate inside the material on the pores surface and be anchored by the orbitals. The separation of these charges can lead to energy storage. However, this state is not stable; therefore, under the certain conditions (such as the certain temperature and/or the certain frequency) this accumulated energy can be emitted [22]. The values of the dielectric loss tangent, which were measured for the manganese-doped BFT-type of ceramics show similar values as for PZT-type ceramic composites [23].

Figure 6 presents Arrhenius plots, namely the logarithm of the relaxation frequency, as a function of the reversal of temperature (Fig. 6a) and the temperature dependencies of the relaxation frequency (Fig. 6b) for the BFT, BFM9T and BFM15T ceramic samples. Using the law of Arrhenius [24], the values of the activation energy were calculated. Calculated activation energies are equal 1.06 eV, 0.54 eV and 0.65 eV, respectively, for BFT, BFM9T and BFM15T ceramic samples. The value of the activation energy calculated for BFT-type materials is consistent with the activation energy values in analogous materials [25].

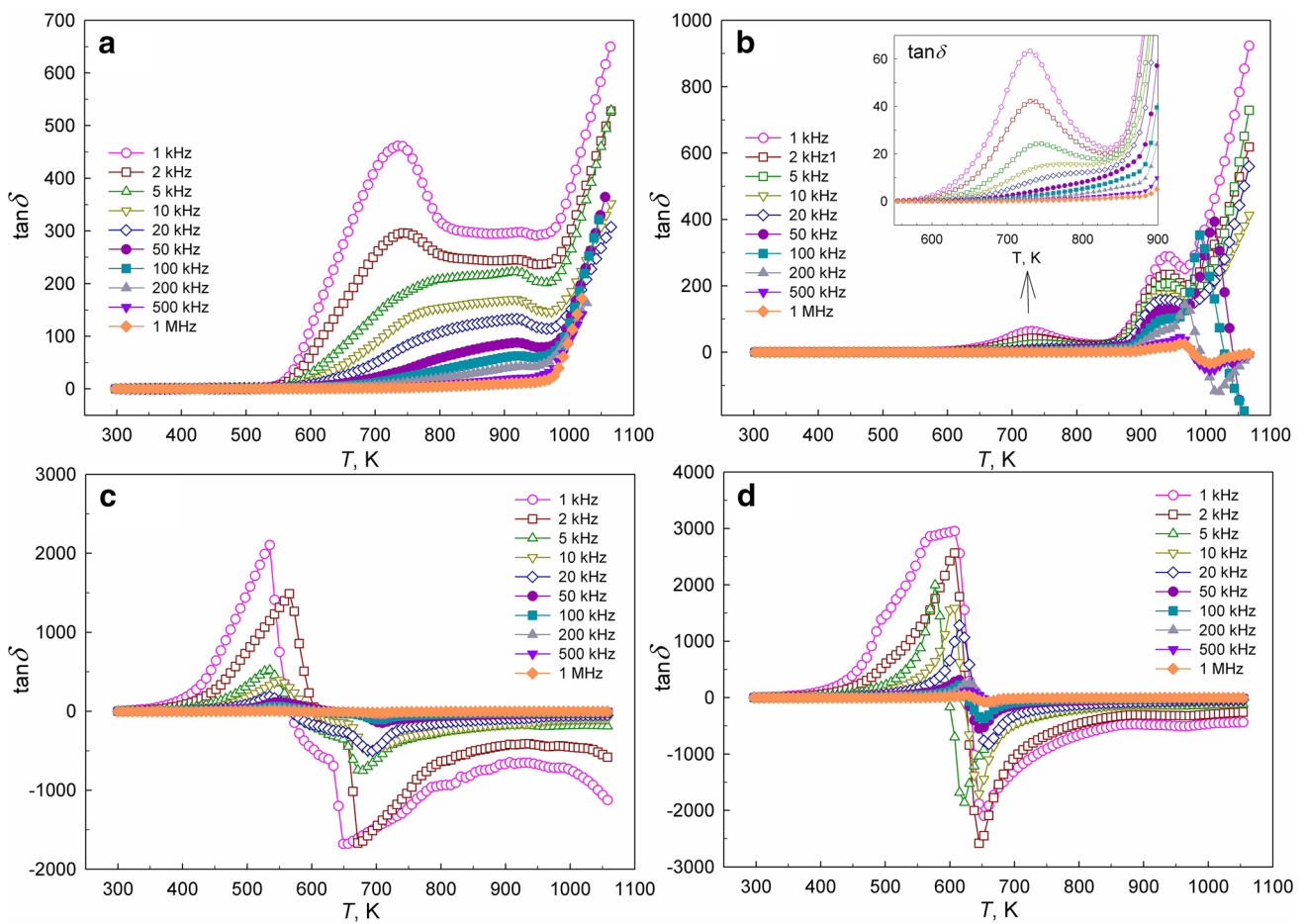


**Fig. 5** Temperature dependencies of dielectric loss tangent for Aurivillius-type ceramic materials: undoped—BFT (a) and doped with manganese: BFM3T (b), BFM9T (c) and BFM15T (d)

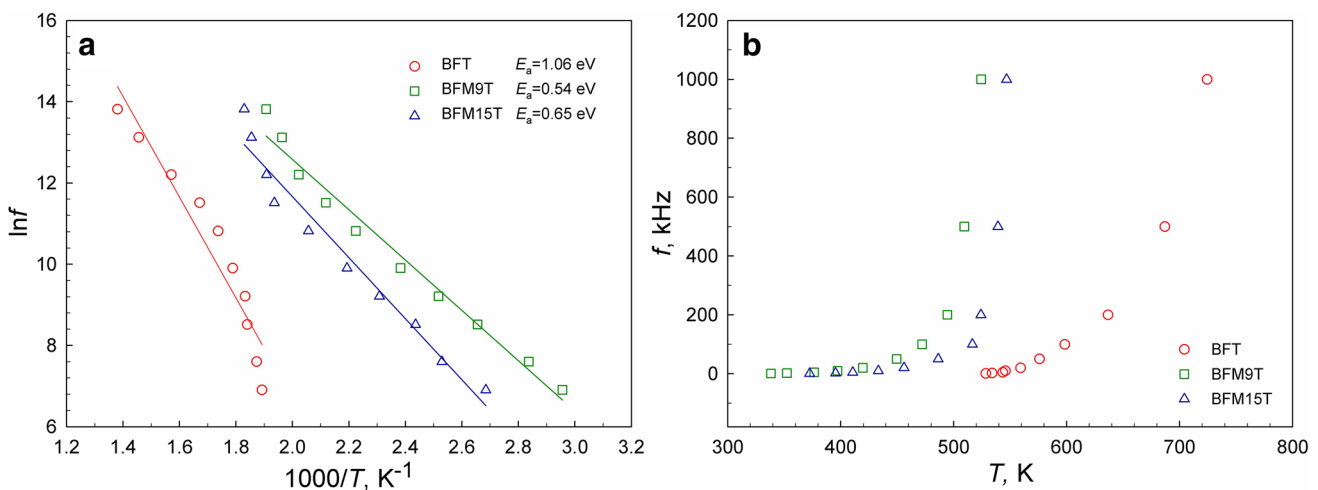


**Fig. 6** The Arrhenius plot of logarithm of relaxation frequency versus temperature (a) and temperature dependence of relaxation frequency (b) for BFT, BFM9T and BFM15. Solid lines are the fitted lines by Arrhenius law

## 4 Conclusions

The materials with the chemical formula:  $\text{Bi}_6\text{Fe}_{2-x}\text{Mn}_x\text{Ti}_3\text{O}_{18}$ , where  $x = 0, 0.3, 0.9, 1.5$  have been designed and successfully obtained. The microstructure and dielectric properties of Mn-doped five-layer Aurivillius-type ceramic were performed.

Based on the research, it was found that increasing the amount of manganese admixture, in the BFT-type materials caused an increase in grain size in morphology of the fracture of the ceramics.

Manganese ions also affected the dielectric properties of these materials. Manganese doping of five-layer Aurivillius-type ceramics activated dielectric relaxation processes. The ceramic material, which did not include manganese ions, showed a positive dielectric constant over the entire temperature range. Manganese doping influenced the change of the electrical character of the tested Aurivillius-type materials and negative values of dielectric constants occur on the temperature dependencies  $\epsilon'(T)$ . A negative value of this physical quantity means that the material polarizes in the opposite direction to the applied external electric field. Materials with such electric properties are called dielectrics by analogy to diamagnetics because the magnetization of diamagnetic materials has opposite direction to the applied external magnetic field. The Mn ion-content in the BFT-type ceramics also has an impact on the value of the dielectric loss tangent. There is a certain amount of the manganese admixture, above which the material begins to exhibit negative dielectric loss.

**Acknowledgements** The authors thank Professor Tomasz Goryczka from the Institute of Materials Science of University of Silesia in Katowice for performing X-ray examinations and many helpful discussions.

## Compliance with ethical standards

**Conflict of interest** The authors declare that they have no conflict of interest.

**Open Access** This article is distributed under the terms of the Creative Commons Attribution 4.0 International License (<http://creativecommons.org/licenses/by/4.0/>), which permits unrestricted use, distribution, and reproduction in any medium, provided you give appropriate credit to the original author(s) and the source, provide a link to the Creative Commons license, and indicate if changes were made.

## References

1. J.A. Bartkowska, R. Zachariasz, D. Bochenek, J. Ilczuk, Arch. Met. Mater. **58**(4), 1401 (2013)
2. J.A. Bartkowska, J. Dercz, J. Exp. Theor. Phys. **117**(5), 875 (2013)
3. B. Aurivillius, Arkiv Kemi **1463**(499), 463 (1949)
4. E.C. Subbarao, J. Am. Ceram. Soc. **45**, 166 (1962)
5. H.J. Kim, J.W. Kim, E.J. Kim, J.Y. Choi, C.M. Raghavan, W.-J. Kim, M.H. Kim, K. Song, J.-W. Kim, S.S. Kim, Ferroelectrics **465**, 68 (2014)
6. Z. Wang, Y. Zhang, Y. Wang, Y. Li, H. Luo, J. Li, D. Viehland, ACS Nano **8**(8), 7793 (2014)
7. S.N. Achary, O.D. Jayakumar, A.K. Tyagi, *Functional Materials* (Elsevier Inc., USA, 2012), p. 159
8. Z. Zhou, N.X. Sun, in *Multiferroic nanostructures*. Composite Magnetolectrics (Elsevier Inc., USA, 2015), p. 71
9. N.J. Joshi, G.S. Grewal, V. Shrinet, T.P. Govindan, A. Pratap, IEEE Trans. Dielectr. Electr. Insul. **19**(1), 83 (2012)
10. A.J.C. Buurma, G.R. Blake, T.T.M. Palstra, U. Adem, *Multiferroic Materials: Physics and Properties* (Elsevier Inc., USA, 2016), p. 1
11. T. Jia, H. Kimura, Z. Cheng, H. Zhao, Sci. Rep. **6**, 31867 (2016). <https://doi.org/10.1038/srep31867>
12. X. Zuo, J. Yang, B. Yuan, D. Song, X. Tang, K. Zhang, X. Zhu, W. Song, J. Dai, Y. Sun, RSC Adv. **4**, 46704 (2014)
13. M. Morawiec, A. Grajcar, J. Achiev. Mater. Manuf. Eng. **80**, 11 (2017)
14. M. Villegas, T. Jardiel, A.C. Caballero, J.F. Fernandez, J. Electroceram. **13**, 543 JF (2004)
15. W. Bai, G. Chen, J.Y. Zhu, J. Yang, T. Lin, X.J. Meng, X.D. Tang, C.G. Duan, J.H. Chu, Appl. Phys. Lett. **100**, 0829021 (2012)
16. K. Tang, W. Bai, J. Liu, J. Yang, Y. Zhang, C.G. Duana, X. Tanga, J. Chu, Ceram. Int. **41**, S185 (2015)
17. B. Yuan, J. Yang, J. Chen, X.Z. Zuo, L.H. Yin, X.W. Tang, X.B. Zhu, J.M. Dai, W.H. Song, Y.P. Sun, Appl. Phys. Lett. **104**, 0624131 (2014)
18. F. Kublel, H. Schmid, Ferroelectrics **129**, 101 (1992)
19. A. Srinivas, D.W. Kim, K.S. Hong, S.V. Suryanarayana, Appl. Phys. Lett. **83**, 2217 (2003)
20. X.Y. Mao, W. Wang, X.B. Chen, Solid State Commun. **147**, 186 (2008)
21. A.K. Srivastava, A.C. Pandey, R. Kripal, S.H. Lee, Soft Mater. **12**, 284 (2014)
22. E. Axelrod, A. Puzenko, Y. Haruvy, R. Reisfeld, Y. Feldman, J. Non Cryst. Solids **352**, 4166 (2006)
23. J.A. Bartkowska, D. Bochenek, J. Mater. Sci. Mater. Electron. **29**(20), 17262 (2018)
24. D. Bochenek, P. Niemiec, P. Guzdek, M. Wzorek, Mat. Chem. Phys. **195**, 199 (2017)
25. H.S. Shulman, D. Damjanovic, N. Setter, J. Am. Ceram. Soc. **83**(3), 528 (2000)